

Structure determination of $c(2 \times 2)$ S on Ni(100) using polarization-dependent surface extended x-ray-absorption fine structure

S. Brennan, J. Stöhr, and R. Jaeger

Stanford Synchrotron Radiation Laboratory, Stanford University, Stanford, California 94305

(Received 23 July 1981)

Improvements in the signal-to-noise ratio of surface extended x-ray-absorption fine-structure spectra of chemisorbed low- Z atoms allow for the first time precise determination of complete adsorption geometries. For $c(2 \times 2)$ S on Ni(100) the first-nearest-neighbor distance is $2.23 \pm 0.02 \text{ \AA}$ and the adsorption site is the fourfold hollow as independently derived from either the second nearest S-Ni distance, amplitude ratios for three polarization directions, or the absolute S coordination number on the surface.

The structural determination of adsorption geometries on surfaces has been limited to low-energy electron diffraction (LEED),¹ photoelectron diffraction (PD),² and surface extended x-ray-absorption fine structure (SEXAFS).^{3,4} The reliability of LEED and PD analysis critically depends on comparison of experimental data to complicated multiple scattering calculations which for LEED has previously lead to discrepancies with SEXAFS data.⁵ SEXAFS has the advantage that it can be analyzed in a theory-independent fashion. However, in the past SEXAFS measurements have often suffered from signal-to-noise problems which have limited the inherent high accuracy of the technique⁶ for structure determinations. Experimental problems were most severe for the technologically most important low- Z atoms where amplitude analysis has previously been unreliable or failed altogether.^{4,5} Here we present SEXAFS results on the low- Z adsorbate sulfur on Ni(100). Besides being the first EXAFS measurements on this important element the present S SEXAFS data exhibit bulklike signal-to-noise ratios and allow the precise determination of the chemisorption site as well as the S-Ni nearest-neighbor distances on the surface. The $c(2 \times 2)$ S on Ni(100) system was chosen because it is regarded as one of the best understood chemisorption systems in surface science with high-quality photoemission,⁷ LEED,^{8,9} and photoelectron diffraction¹⁰ data as well as theoretical calculations¹¹ being available. The present SEXAFS data thus allow a critical assessment of the reliability and accuracy of the various surface structural techniques in use and demonstrate convincingly that SEXAFS yields the most precise structural information for adsorbate complexes.

We find a S-Ni first-nearest-neighbor distance of $2.23 \pm 0.02 \text{ \AA}$, the accuracy being limited only by the EXAFS technique itself. For normal x-ray incidence the second-nearest-neighbor distance to Ni atoms in the (100) surface plane is clearly observed, and its distance of $4.15 \pm 0.10 \text{ \AA}$ determines the adsorption

site to be the fourfold hollow. This site is independently confirmed from analysis of the polarization-dependent nearest-neighbor SEXAFS amplitudes (relative amplitude ratios) and thirdly from determination of the *absolute* S coordination number on the surface by comparison with a bulk NiS standard.

Experiments were performed using synchrotron radiation from the double crystal monochromator Jumbo¹² at the Stanford Synchrotron Radiation Laboratory. With Ge(111) crystals this ultrahigh-vacuum-compatible monochromator transmits radiation in the 2000–4000-eV range with ~ 1.5 -eV resolution and a flux of $\sim 10^{11}$ photons/sec at the sulfur K edge (~ 2472 eV). Spectra were recorded using a cylindrical mirror analyzer (CMA) in the nonretarding mode. The kinetic energy window of ~ 30 -eV width was centered at 2100 eV, the S KLL Auger energy. This allowed measurement of the SEXAFS signal for ~ 400 eV past the K edge before the Ni $2p$ photoelectrons swept into the CMA energy window. The SEXAFS spectra were flux normalized by a reference monitor consisting of a Cu grid and a spiraltron electron multiplier.¹³ Data were taken at room temperature at x-ray incidence angles θ of 90° , 45° , and 10° with respect to the surface. The Ni(100) crystal ($\sim \frac{5}{8}$ -in. diameter) was cleaned using Ar^+ bombardment and oxygen heat treatments to produce a surface with less than 1% of C, O, and S. The clean annealed surface was dosed with H_2S and was characterized by Auger electron spectroscopy and LEED.

Figure 1 shows the raw S K -edge SEXAFS spectrum taken at room temperature and $\theta = 45^\circ$ and the background-subtracted SEXAFS oscillations underneath. The oscillations are visible with good signal-to-noise contrast out to 400 eV past the edge (2472 eV). The beating in frequency due to the second-nearest-neighbor shell is also visible. The amplitude envelope of the oscillations is indicative of the Z of the backscattering Ni atoms. Before Fourier transformation, the EXAFS $\chi(k)$ signal was multiplied by k^2 , and each spectrum was normalized to its edge jump,

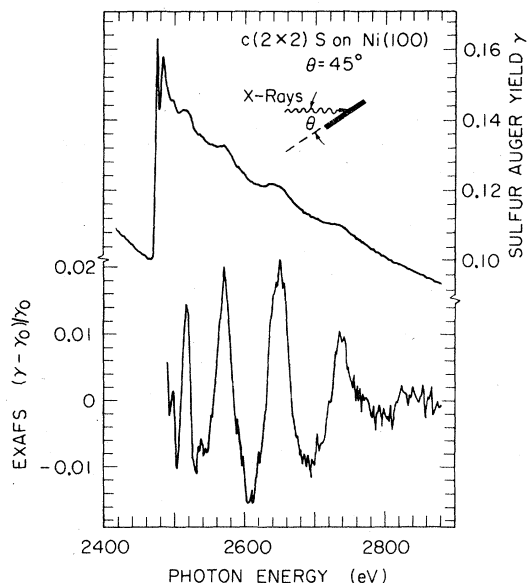


FIG. 1. Sulfur K -edge SEXAFS spectrum for $c(2 \times 2)$ (half monolayer) S on Ni(100) recorded at 45° x-ray incidence. The SEXAFS oscillations after background subtraction are shown in the lower half.

to give a basis for the amplitude comparison. In Fig. 2 both the magnitude and the imaginary part of the Fourier transform are shown for normal x-ray incidence ($\theta = 90^\circ$). Peak *A* corresponds to the S-Ni nearest-neighbor distance and peak *B* to the S-Ni second-nearest-neighbor distance for Ni atoms in the (100) surface plane.

For distance analysis we used a phase shift obtained from bulk NiS EXAFS spectra taken in the to-

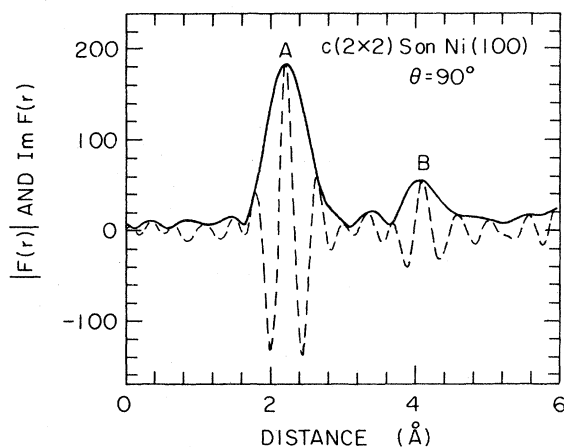


FIG. 2. Absolute value (solid line) and imaginary part (dashed) of the Fourier transform of the SEXAFS signal for $c(2 \times 2)$ S on Ni(100) recorded at $\theta = 90^\circ$.

TABLE I. S-Ni nearest-neighbor distances for $c(2 \times 2)$ S on Ni(100).

θ^a (deg)	S-Ni nearest-neighbor distance (\AA)	S-Ni second-nearest-neighbor distance ^b (\AA)
10	2.24 ± 0.02	
45	2.23 ± 0.02	
90	2.23 ± 0.02	4.15 ± 0.10

^a See Fig. 1.

^b For Ni atoms in the surface plane.

tal yield mode. The S-Ni distance in NiS (NiAs structure) is accurately known to be $(2.3944 \pm 0.0003) \text{\AA}$.¹⁴ Table I summarizes the results of the neighbor distance determinations for three angles of incidence. All three SEXAFS spectra yielded a S-Ni nearest-neighbor distance within 0.01\AA using both the analysis methods of the Lee and Beni¹⁵ and Martens *et al.*¹⁶ Including all sources of errors we conservatively quote the S-Ni distance on the surface to be $2.23 \pm 0.02 \text{\AA}$, or $0.16 \pm 0.02 \text{\AA}$ shorter than for bulk NiS.

The S chemisorption site can be determined from the observed second-neighbor distance alone. For $\theta = 90^\circ$ we observe a second-shell distance at $4.15 \pm 0.10 \text{\AA}$ (cf. Fig. 2). This value can now be compared to that expected for different chemisorption sites. Using 2.23\AA for the nearest-neighbor S-Ni distance we can calculate where the most pronounced higher-neighbor peak should fall. We obtain 4.17\AA for the fourfold hollow, 3.34\AA for the bridge, and 3.34\AA for the top sites, respectively. Furthermore, the top site, because the first-nearest-neighbor Ni atom is directly below, should show no EXAFS at normal incidence ($\theta = 90^\circ$), in conflict with experiment. Therefore, the prominent second-nearest-neighbor peak at $4.15 \pm 0.10 \text{\AA}$ unambiguously determines the fourfold hollow as the adsorption site.

The fourfold site is independently determined from comparison of experimental and calculated polarization-dependent SEXAFS amplitude ratios. The ratio of the amplitudes obtained from the back-transformed filtered first-nearest-neighbor-shell peak *A* (Fig. 2) for different angles θ directly yields the ratio of effective coordination numbers for S on Ni(100). Since the same sample is measured in all cases, all problems with amplitude transferability^{17,18} between chemically inequivalent systems are eliminated. For K edges the effective coordination number N^* of the absorbing atom is given by⁴

$$N^* = 3 \sum_{i=1}^N \cos^2 \alpha_i, \quad (1)$$

TABLE II. Experimental versus calculated coordination numbers and ratios for $c(2 \times 2)$ S on Ni(100).

Incidence angle (deg)	Expt.	Fourfold hollow	Twofold bridge	Onefold atop
10/90	1.16 ± 0.10	1.20	4.31	∞
10/45	1.15 ± 0.10	1.09	1.59	1.94
10	4.42 ± 1.04^a	4.49	4.03	2.91
45	3.77 ± 0.79^a	4.13	2.53	1.50
90	3.94 ± 0.75^a	3.75	0.94	0

^a Relative to $N=6$ for bulk NiS.

where N is the number of neighbors in a given shell and α_i is the angle between the electric field vector \vec{E} and a vector pointing from the absorbing atom to the i th atom in that shell. SEXAFS studies on K edges offer the distinct advance over $L_{2,3}$ edges¹⁹ that the anisotropy in N^* is considerably larger.⁶ Thus, in most cases the chemisorption site can be determined solely by comparing measured and calculated N^* ratios for different \vec{E} vector orientations (angles of incidence θ).

For our data analysis a Fourier window function was chosen which yielded a constant nearest-neighbor distance and a constant amplitude ratio as a function of k . The derived experimental amplitude ratios are shown in Table II, along with the calculated effective coordination numbers and their ratios for the three most likely models for S on the (100) surface. The atop site is ruled out since no EXAFS should be observed for $\theta=90^\circ$. The twofold bridge model can also be eliminated since the EXAFS should be more than a factor 4 larger at 10° than at 90° incidence. The experimentally determined ratio for $N^*(10^\circ)/N^*(90^\circ)$ is 1.16 ± 0.10 , less than 4% from the theoretical value for the fourfold site. The accuracy of our relative amplitude determination was found to be better than $\pm 10\%$ by comparing each *two* sets of data taken at 10° , 45° , and at 90° . This is comparable to the accuracy with which bulk EXAFS data can be analyzed.^{17,18}

Finally, we can compare the SEXAFS amplitudes to that obtained for our bulk NiS standard for which each S atom is known to be surrounded by six Ni atoms. Using standard analysis procedures,⁴ we can derive an *absolute* effective coordination number $N^*(\theta)$ for S on Ni(100) which can then be compared to the $N^*(\theta)$ value calculated for an assumed site from Eq. (1). As shown in Table II, this procedure,

as a third independent determination, again favors the fourfold hollow site. These last results strongly support the conclusions on amplitude transferability drawn previously¹⁹ for the high- Z atom iodine on Cu surfaces. Our absolute coordination numbers determined from experiment are all within 10% of the calculated N^* values for the fourfold hollow. Because of phase-shift transferability limitations between bulk and surface the experimental error bars are, however, about twice ($\sim 20\%$) as large as for the relative amplitude ratios of the surface spectra.

The present Communication demonstrates the state-of-the-art reliability and accuracy of SEXAFS on low- Z adsorbates on surfaces and of SEXAFS as a technique in general. Our results are in good agreement with theory,¹¹ LEED,^{8,9} and photoelectron diffraction¹⁰ but are superior in that they provide better accuracy for the S-Ni bond length (2.23 ± 0.02 Å). In comparison the LEED value^{8,9} of $d_{11} = (1.3 \pm 0.1)$ Å corresponds to a S-Ni distance of 2.19 ± 0.06 Å. It appears that the present study points the way for precise structure determinations of the important low- Z atoms on surfaces.

We would like to thank E. Umbach, R. Treichler, and K. Baberschke for experimental help during the initial phase of the project. One of us (S.B.) would like to acknowledge P.H. Citrin for many helpful discussions. All of the materials incorporated in this work were developed at the Stanford Synchrotron Radiation Laboratory which is supported by the National Science Foundation (under Contract No. DMR77-27489), in cooperation with SLAC and the Department of Energy. One of us (R.J.) would like to thank the Eastman Kodak Company and the Deutsche Forschungsgemeinschaft for supporting his work at SSRL.

- ¹See, for example, F. Jona, *J. Phys. C* **11**, 4271 (1978).
- ²S. D. Kevan, D. H. Rosenblatt, D. Denley, B. C. Lu, and D. A. Shirley, *Phys. Rev. Lett.* **41**, 1565 (1978).
- ³P. H. Citrin, P. Eisenberger, and R. C. Hewitt, *Phys. Rev. Lett.* **44**, 309 (1978).
- ⁴J. Stöhr, L. I. Johansson, I. Lindau, and P. Pianetta, *Phys. Rev. B* **20**, 664 (1979).
- ⁵L. I. Johansson and J. Stöhr, *Phys. Rev. Lett.* **43**, 1882 (1979); J. Stöhr, L. I. Johansson, S. Brennan, M. Hecht, and J. N. Miller, *Phys. Rev. B* **22**, 4052 (1980).
- ⁶See, for example, S. Heald and E. A. Stern, *Phys. Rev. B* **17**, 4069 (1978).
- ⁷E. W. Plummer, B. Tonner, N. Holzwarth, and A. Liebsch, *Phys. Rev. B* **21**, 4306 (1980).
- ⁸J. E. Demuth, D. W. Jepsen, and P. M. Marcus, *Phys. Rev. Lett.* **31**, 540 (1973); **32**, 1182 (1974).
- ⁹Y. Gauthier, D. Aberdam, and R. Baudouin, *Surf. Sci.* **78**, 339 (1978), and references therein.
- ¹⁰D. H. Rosenblatt, J. G. Tobin, M. G. Mason, R. F. Davis, S. D. Kevan, D. A. Shirley, C. H. Li, and S. Y. Tong, *Phys. Rev. B* **8**, 3828 (1981).
- ¹¹S. P. Walch and W. A. Goddard, III, *Surf. Sci.* **72**, 645 (1978).
- ¹²J. Cerino, J. Stöhr, N. Hower, and R. Z. Bachrach, *Nucl. Instrum. Methods* **172**, 227 (1980).
- ¹³J. Stöhr, R. Jaeger, J. Feldhaus, S. Brennan, D. Norman, and G. Apai, *Appl. Opt.* **19**, 3911 (1980).
- ¹⁴J. Trahan, R. G. Goodrich, and S. F. Watkins, *Phys. Rev. B* **2**, 2859 (1970).
- ¹⁵P. A. Lee and G. Beni, *Phys. Rev. B* **15**, 2862 (1977).
- ¹⁶G. Martens, P. Rabe, N. Schwentner, and A. Werner, *Phys. Rev. B* **17**, 1418 (1978).
- ¹⁷E. A. Stern, B. A. Bunker, and S. M. Heald, *Phys. Rev. B* **21**, 5521 (1980).
- ¹⁸P. Eisenberger and B. Lengeler, *Phys. Rev. B* **22**, 3551 (1980).
- ¹⁹P. H. Citrin, P. Eisenberger, and R. C. Hewitt, *Phys. Rev. Lett.* **45**, 1948 (1980).